Control Design for Electronic Voltage Stabilizer

Nguyen Thi Diep
Faculty of Control and Automation, Electric Power University, Vietnam
diepnt@epu.edu.vn

Doan Hong Quan
Faculty of Control and Automation, Electric Power University, Vietnam
doanhongquanepu@gmail.com

Nguyen Huu Minh
School of Electrical and Electronic Engineering, Hanoi University of Science and Technology, Vietnam
minh.nh191962@sis.hust.edu.vn

Nguyen Kien Trung
School of Electrical and Electronic Engineering, Hanoi University of Science and Technology, Vietnam
trung.nguyenkien1@hust.edu.vn (corresponding author)

Received: 15 August 2024 | Revised: 13 October 2024, 30 October 2024, and 4 November 2024 | Accepted: 21 November 2024

 DOI: https://doi.org/10.48084/etasr.8749

ABSTRACT

Vietnam's electrical infrastructure has undergone notable advancements in recent times. Nevertheless, concerns pertaining to under-voltage, over-voltage, and voltage fluctuations persist in rural, mountainous, and industrial regions. This results in the inefficient operation of electrical equipment, disruptions in industrial production processes, data loss, and equipment damage. This paper puts forth a novel control design methodology for electronic voltage stabilizers, with the objective of mitigating the detrimental effects of grid voltage fluctuations on electrical apparatus. A compact and cost-effective AC-AC converter is proposed as a means of regulating the compensation voltage. The paper puts forth the use of the state-space averaging method for system modeling and proposes the combination of feedback and feed-forward controllers to achieve high accuracy and rapid response times. Furthermore, the moving average method is proposed for measuring the Root Mean Square (RMS) voltage, which significantly enhances the control response speed and accuracy. A 10 kVA single-phase electronic voltage stabilizer was constructed and tested in a laboratory setting under a range of grid voltage conditions, from 150V to 290V, and with varying loads. The results demonstrate that the electronic voltage stabilizer is effective in maintaining the load voltage within the desired range. The maximum response time recorded was found to be half a cycle of the grid voltage in the simulation and one cycle in the experiments, which is a significantly faster response time than that of similar designs. Furthermore, the low total harmonic distortion provides additional confirmation of the effectiveness of the designed electronic voltage stabilizer.

Keywords-electromagnetic voltage stabilizer; electronic voltage stabilizer; AC-AC converter; feed-forward controller; feed-back controller

I. INTRODUCTION

The operational lifespan and efficiency of electrical equipment can be adversely affected by under-voltage, over-voltage, and fluctuating voltage. These issues result in inefficient operation, disruption to the production process, loss of important data, and even damage to equipment [1-6]. There are numerous factors that can contribute to voltage instability at the source, including geographical location, the quality of the transmission system, the initiation of high-capacity loads, the occurrence of short circuits, the failure of the power system, and the occurrence of peak hour overloads. In order to address these challenges, a number of solutions have been proposed with the aim of monitoring, protecting, and stabilizing voltage at various points within the power system, including the transmission system, terminals and loads [7-9]. One of the most frequently proposed solutions for stabilizing voltage for electrical equipment is the use of a voltage stabilizer. The objective of these devices is to mitigate the adverse effects of source voltage instability on electrical equipment. The majority of voltage stabilizers currently available on the market are electromagnetic in nature, typically comprising an autotransformer and a servo motor. These stabilizers are valued for their simplicity, reliability, and ability to provide a less distorted output voltage with a wide range of voltage adjustments. However, the carbon brush system has been

identified as a source of noise and wear during operation, exhibiting a slow response time due to mechanical impact, and is unsuitable for use in explosive environments due to the potential for arc formation during brush movement [10-13]. Moreover, an Uninterruptible Power Supply (UPS) can be employed for the purpose of voltage stabilization. Online UPS systems are designed to maintain a stable output voltage in the event of fluctuations in the input voltage, even in the absence of a power supply for a designated period of time [14, 15]. Nevertheless, the intricate configuration of online UPS systems inevitably entails a substantially elevated financial outlay in comparison to alternative voltage stabilizer devices.

In recent times, there have been proposals for the use of voltage stabilizer structures that employ power electronic converters with a view to achieving enhanced accuracy and more rapid response times. These advanced structures typically include power electronic converters and compensation transformers, offering significant advantages over traditional electromagnetic voltage stabilizers. These advantages include rapid response times, high accuracy, the absence of noise, abrasion, sparks, and a reduction in maintenance requirements [16-20]. In comparison to an online UPS, an electronic voltage stabilizer exhibits a more straightforward configuration, a greater degree of reliability, and a substantially more cost-effective profile. Authors in [16], proposed an AC-AC converter and compensation transformer as means of managing voltage fluctuations, such as sags or swells in the source voltage. However, the study does not include an analysis of a closed-loop controller, which may result in a reduction in control accuracy. Authors in [17] presented a study in which an AC-AC buck converter is employed in series with a transformer for the purpose of voltage compensation. The structure is characterized by a relatively simple hardware configuration. However, the use of a PI controller may result in a slower response time. Authors in [18, 19], used a series compensating transformer and an AC-AC converter, with a linear quadratic regulator and anti-windup to regulate the output voltage of the AC-AC converter. However, this control structure relies on a model transformation from a fixed coordinate system to a rotating coordinate system, which increases the control calculation time. Authors in [20] employed a dual-buck-type buck-boost AC-AC converter for voltage compensation. This structure offers the advantage of no short-circuit and open-circuit and can achieve soft switching without RC snubbers. Authors in [21], designed two H-bridge structures to regulate voltage fluctuations, including swell and sag. The first structure serves as a rectifier, while the second is employed as an inverter. Authors in [22], composed a buck-boost converter of eight switches, four inductors, and two capacitors, with a minimum of three switches operating in each cycle. However, these structures are relatively complex and require multiple converters and passive components, which results in increased size and losses.

This paper puts forth a control design method for an electronic voltage stabilizer comprising an AC-AC converter, a compensation transformer, and an H-bridge TRIAC for the purpose of inverting the compensation voltage phase. The AC-AC converter is both compact and cost-effective, as its sole function is to regulate the compensation voltage amount. The system is modeled using the state-space averaging method, and feed-forward and feedback controllers are designed to ensure high accuracy and rapid response times. Furthermore, the moving average method is deployed to ascertain the RMS value of the voltage, thereby enhancing the system's response speed and accuracy. The proposed control design results in a voltage stabilizer with superior response time and accuracy compared to other designs.

II. THEORETICAL BASIS

A. Proposed System Structure Analysis

Figure 1 presents the proposed configuration of an electronic voltage stabilizer. The system permits fluctuations in the load voltage within a range of 5% of the reference voltage. In the event that the source voltage is within the range of 210 V AC to 230 V AC, the AC-AC converter is rendered inactive, with the load being directly connected to the source via T5. In the event of a deviation in the source voltage from the specified range, the AC-AC converter is triggered to generate the requisite compensation voltage, which is then conveyed through the compensation transformer to guarantee the delivery of an accurate voltage to the load. The function of the TRIACs (T1, T2, T3, and T4) is to alter the phase of the compensation voltage. The phase angle on the secondary coil of the compensation transformer is modified by switching the TRIAC pairs (T1 and T2 and T3 and T4). This mechanism enables the voltage stabilizer to maintain a stable voltage when the source voltage is outside the reference range.

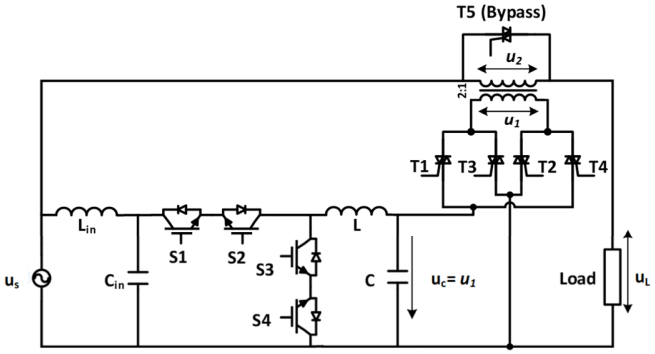

Fig. 1. Proposed structure of an electronic voltage stabilizer.

The AC-AC converter comprises four Insulated-Gate Bipolar Transistors (IGBTs) (S1, S2, S3, and S4) and two input/output LC filters, enabling direct AC-AC conversion without the necessity for a DC stage. This differs from the configuration of a traditional inverter structure. The output voltage of the AC-AC converter is regulated through Pulse Width Modulation (PWM), as shown in Figure 2. During the positive half-cycle of the source voltage, the S2 and S4 switches are continuously on, while the S1 and S3 switches are controlled by the PWM signal, turning on alternately. Upon the activation of S1, the current from the source is directed through S1, S2, and the filter (L), thereby supplying the load, which is the primary coil of the compensation transformer, as presented in Figure 3 (a). Upon the activation of S3, the load current is sustained through the participation of both S3 and S4, as

depicted in Figure 3 (b). During the negative half-cycle of the supply voltage, the AC-AC converter operates in a manner analogous to that previously described. This operation is analogous to that of a buck converter, but applied to the AC power.

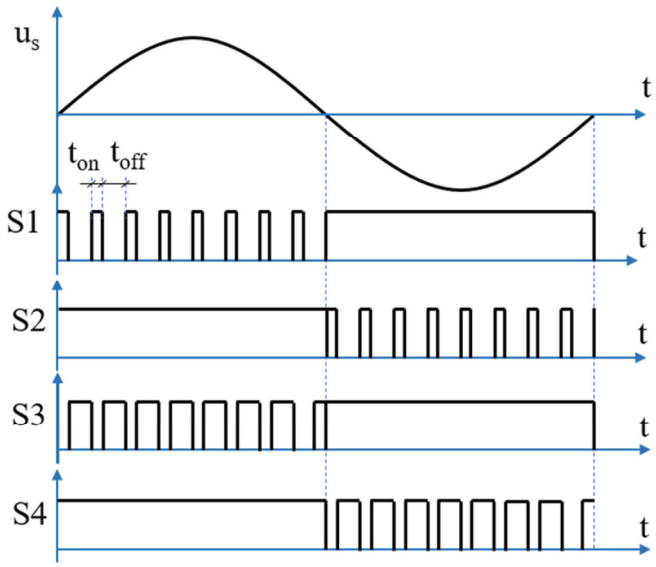

Fig. 2. PWM modulation signals.

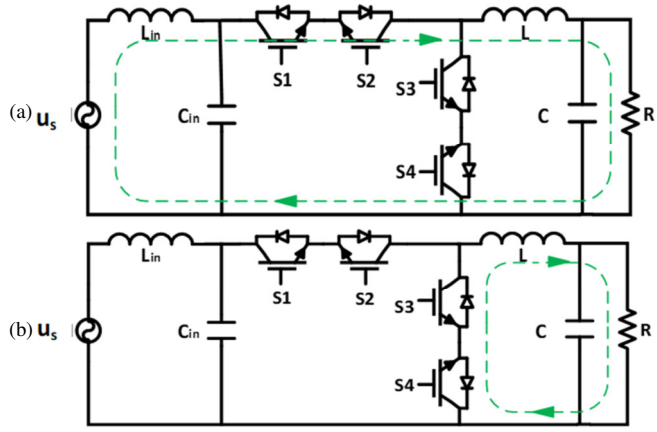

Fig. 3. Equivalent diagram: (a) when S1 is on, (b) when S3 is on.

The principle of voltage compensation is performed as follows: When the source voltage is lower than the reference voltage (ranging from 150 V AC to 210 V AC), T1 and T2 are activated, while T3 and T4 remain deactivated. This results in the source voltage and the compensation voltage being in phase, thereby ensuring that the load voltage is equal to the sum of the source voltage and the compensation voltage:

$$u_L = u_s + u_2 \quad (1)$$

where u_L is the load voltage, u_s is the source voltage, and u_2 is the secondary voltage of the compensation transformer. When the source voltage is greater than the reference voltage, the T1 and T2 switches are deactivated, while the T3 and T4 switches are activated. This results in a phase shift between the source voltage and the compensation voltage, with the load voltage becoming equal to the source voltage minus the compensation voltage:

$$u_L = u_s - u_2 \quad (2)$$

The on/off signals of IGBTs and TRIACs follow the rules, as depicted in Table I.

TABLE I. THE ON/OFF SIGNALS OF IGBTS AND TRIACS

Mode	Phase	IGBT				TRIAC			
		S1	S2	S3	S4	T1	T3	T2	T4
Low voltage	+	1	1	0	1	1	0	1	0
		0	1	1	1	1	0	1	0
	-	1	1	1	0	1	0	1	0
		1	0	1	1	1	0	1	0
High voltage	+	1	1	0	1	0	1	0	1
		0	1	1	1	0	1	0	1
	-	1	1	1	0	0	1	0	1
		1	0	1	1	0	1	0	1

B. System Modeling

It is reasonable to assume that the source voltage can be represented as a sinusoidal function, indicated by:

$$u_s = U_{sm} \sin(\omega t) \quad (3)$$

where U_{sm}, ω are respectively the amplitude and angular frequency of the source voltage. Because the state space average model is based on the switching cycle (T_s), and the switching frequency is much larger than the grid frequency (50 Hz). So, in a switching cycle, the value has a smaller frequency than being considered a constant. The output voltage of the AC-AC converter is:

$$u_c = D \times U_{sm} \sin(\omega t) + \sum_0^{\infty} \frac{D \times U_{sm} \sin(kD\pi)}{k\pi} \sin(k\omega_s \pm \omega)t \quad (4)$$

$$D = \frac{t_{on}}{t_{on}+t_{off}} \quad (5)$$

where D is the modulation coefficient, ω_s is the PWM frequency, $t_{on}; t_{off}$ are the times for turning on and off switch S1, respectively. Considering that the output filter (L, C) will fully absorb the generated harmonic component. Thus, u_c will only have the fundamental wave component.

$$u_c = D \times U_{sm} \sin(\omega t) = D \times u_s \quad (6)$$

During the initial phase of the source voltage (positive half cycle), switches S1 and S3 are activated in an opposing manner, while switches S2 and S4 remain continuously active. This pattern reverses during the subsequent half cycle. Pairs S1 and S2 are equivalent to switch K1, while pairs S3 and S4 are equivalent to switch K2. The on/off states of switches K1 and K2 are opposite during the operational period. The equivalent diagram of an AC-AC converter in a positive half cycle of the source voltage is shown in Figure 4. In this context, R represents the equivalent load impedance observed from the input side of the compensation transformer to the load. In the initial state, K1 is activated while K2 is deactivated, as

presented in Figure 4 (b). The mathematical expressions that describe the circuit are:

$$\begin{cases} L\frac{di_1(t)}{dt} = u_s(t) - u_c(t) \\ C\frac{du_c(t)}{dt} = i_1(t) - i_3(t) \\ u_c(t) = Ri_3(t) \end{cases} \quad (7)$$

In the second state, the K1 component is deactivated, while the K2 component is activated, as can be seen in Figure 4 (c). The relationships between the circuit components are expressed by:

$$\begin{cases} L\frac{di_1(t)}{dt} = -u_c(t) \\ C\frac{du_c(t)}{dt} = i_1(t) - i_3(t) \\ u_c(t) = Ri_3(t) \end{cases} \quad (8)$$

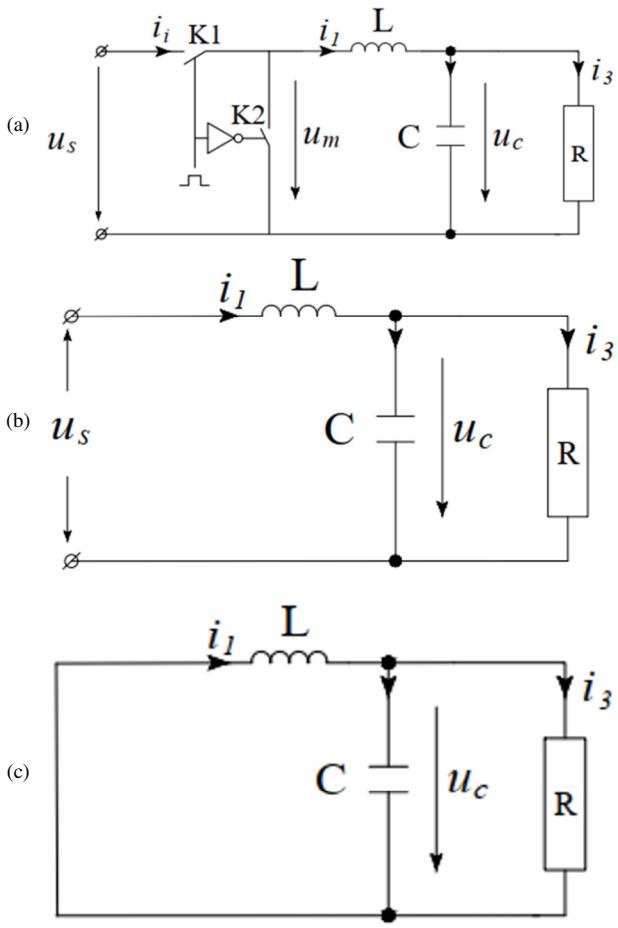

Fig. 4. Equivalent circuit of AC-AC converter in a positive half cycle of source voltage: (a) general equivalence diagram, (b) state 1: K1 turns on and K2 turns off, (c) state 2: K1 turns off and K2 turns on.

Because K1 and K2 turn on/off with opposite states, choose the switch function as:

$$\begin{cases} h = 1 \; when \; K_1 \; turn \; on \; and \; K_2 \; turn \; off \\ h = 0 \; when \; K_1 \; turn \; off \; and \; K_2 \; turn \; on \end{cases}$$

Therefore, the system of equations describing the circuit is:

$$\begin{cases} L\frac{di_1(t)}{dt} = h.u_s(t) - u_c(t) \\ C\frac{du_c(t)}{dt} = i_1(t) - \frac{u_c(t)}{R} \end{cases} \quad (9)$$

During a switching cycle, the switching function is averaged $h_{T_s} = d$, and the averaging model is obtained as:

$$\begin{cases} L\frac{d\langle i_1(t)\rangle_{T_s}}{dt} = d.\langle u_s(t)\rangle_{T_s} - \langle u_c(t)\rangle_{T_s} \\ C\frac{d\langle u_c(t)\rangle_{T_s}}{dt} = \langle i_1(t)\rangle_{T_s} - \frac{\langle u_c(t)\rangle_{T_s}}{R} \end{cases} \quad (10)$$

In a steady working state:

$$\begin{cases} U_{cm} = DU_{sm} \\ I_{1m} = D\frac{U_{sm}}{R} \end{cases} \quad (11)$$

The system of equations with small fluctuating variables is represented as:

$$\begin{cases} L\frac{d\tilde{\imath}_{1m}(t)}{dt} = U_{sm}\tilde{d}(t) + D\tilde{u}_{sm}(t) - \tilde{u}_{cm}(t) \\ C\frac{d\tilde{u}_{cm}(t)}{dt} = \tilde{\imath}_{1m}(t) - \frac{\tilde{u}_{cm}(t)}{R} \end{cases} \quad (12)$$

Transform to the Laplace domain:

$$\begin{cases} sL\tilde{\imath}_{1m}(s) = U_{sm}\tilde{d}(s) + D\tilde{u}_{sm}(s) - \tilde{u}_{cm}(s) \\ sC\tilde{u}_{cm}(s) = \tilde{\imath}_{1m}(s) - \frac{\tilde{u}_{cm}(s)}{R} \end{cases} \quad (13)$$

Because the $f_s \gg f_{sm}$, assuming the source voltage is constant in one switching cycle, the transfer function between the converter output voltage and the modulation coefficient D is obtained as:

$$G_{u_c d}(s) = \frac{\tilde{u}_{cm}(s)}{\tilde{d}(s)} = \frac{U_{sm}}{LCs^2 + \frac{L}{R}s + 1} \quad (14)$$

C. Measurement Algorithms and Control Design

The control structure has been designed in accordance with the parameter of the effective value of voltage. In this system, there is a delay in measuring the RMS value of the load and source voltages, which affects the feedback controller's response. Therefore, a feed-forward controller is combined with a feedback controller so that the load voltage quickly returns to the safe operating point for the load. The feed-forward controller offers a fast response, while the feedback controller can eliminate static errors. The block diagram of the system's control structure is displayed in Figure 5.

1) Feed Forward Controller Design

When the source voltage is less than the reference voltage ($U_s < U_{ref}$):

$$\begin{cases} D = D_f + D_{fk} \\ U_L = U_s + U_2 \end{cases} \quad (15)$$

When the source voltage is greater than the reference voltage ($U_s > U_{ref}$):

$$\begin{cases} D = D_f - D_{fk} \\ U_L = U_s - U_2 \end{cases} \quad (16)$$

where U_{ref} is the reference voltage. To make the output voltage equal to the reference voltage, the amount of voltage that needs to be compensated or subtracted is:

$$U_2 = |U_{ref} - U_s| \quad (17)$$

With the selected transformer coefficient (k) equal to $\frac{1}{2}$, the required output voltage of the AC-AC converter is:

$$U_c = U_1 = \frac{U_2}{k} = 2|U_{ref} - U_s| \quad (18)$$

The modulation coefficient of the Feed-forward is calculated as:

$$D_f = 2\frac{|U_{ref} - U_s|}{U_s} \quad (19)$$

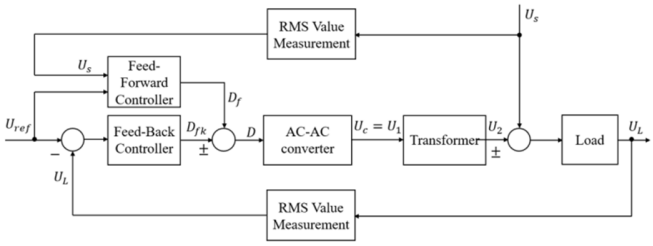

Fig. 5. Block diagram of the system's control structure.

2) Feed Back Controller Design

The transfer function of the control object is determined from (14) as:

$$G(s) = \frac{\tilde{u}_{2m}(s)}{\tilde{d}(s)} = \frac{1}{2}\frac{U_{sm}}{LCs^2 + \frac{L}{R}s + 1} \quad (20)$$

where $U_s = 220\ \text{V}, L = 1.5\ \text{mH}, C = 10\ \mu\text{F}, R = 6.16\ \Omega$.

The Bode plot of the object is shown in Figure 6. The feedback controller is calculated by:

$$C(s) = \frac{0.8195s + 12890}{s} \quad (21)$$

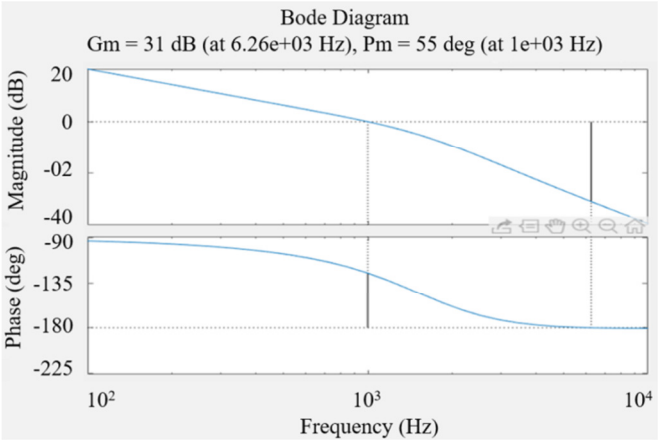

Fig. 6. Bode plot of the object when there is a PI controller.

3) RMS Value Measurement Algorithm

The system parameters are calculated based on the RMS measurement value of the source and output voltage. The measurement signal sampling process is illustrated in Figure 7. The RMS value is calculated by:

$$TrueRMS = \sqrt{\frac{\sum_1^n V_n^2}{n}} = \sqrt{\frac{\overline{RMS^2}sin^2(\alpha_1) + \overline{RMS^2}sin^2(\alpha_2) \ldots + \overline{RMS^2}sin^2(\alpha_n)}{n}}$$

$$= \sqrt{\frac{n.\overline{RMS^2} + \overline{RMS^2}[cos(\alpha_1 - \alpha_x).\cos(\alpha_1 + \alpha_x) + \cdots]}{n}} = \overline{RMS} \quad (22)$$

$$\alpha_1 - \alpha_x \sim 90^0 \ or \ \cos(\alpha_1 - \alpha_x) \sim 0 \quad (23)$$

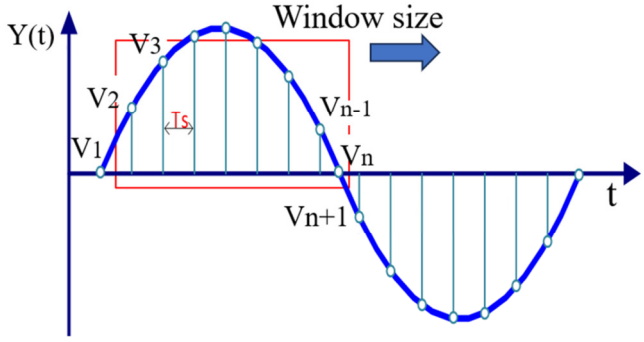

Fig. 7. Measurement signal sampling process.

The sampling frequency should be selected to be equal to the control frequency. The input sine signal is sampled with an even number of samples to generate signal pairs (α_1 and α_x) that satisfy the condition in (23), thereby cancelling the cosine component in (22) and obtaining the RMS value. The measurement signal is updated continuously using the moving average method (replacing the oldest sample with a new one in the sample frame). This method for measuring and calculating the RMS value provides a rapid response time, approximately half of the grid voltage cycle. The algorithm's precision for measuring the RMS value of the voltage on the Matlab-Simulink simulation has been validated, and the results are presented in Figure 8. The measured value is in close agreement with the actual value, with an error of less than 1%. The response time is rapid, occurring at a rate of approximately half the grid voltage cycle, or less than 0.01 seconds. The results presented herein demonstrate the feasibility of the measurement method and its potential applicability to electronic voltage stabilizers.

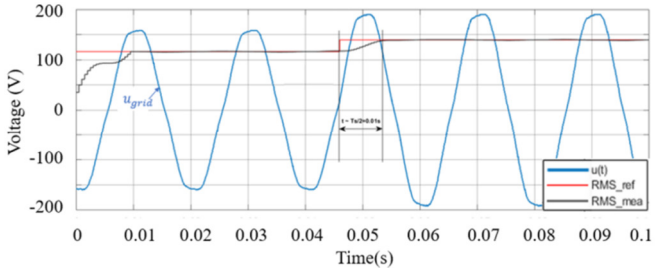

Fig. 8. Response of measurement algorithm to 50 Hz source voltage.

III. SIMULATION AND EXPERIMENTAL RESULTS

A. Simulation Results

A Matlab-Simulink simulation model was developed for the purpose of verifying the accuracy of the proposed method. To assess the performance of the electronic voltage stabilizer, simulations were conducted using four representative grid voltage fluctuations at full load (10 kVA). The simulations included a variety of common loads, including resistive, RL, RC, and the most severe nonlinear bridge rectifier loads with large DC capacitors. In the graphic results, the reference voltage is represented by the red dashed line, the grid voltage is displayed by the blue line, and the load voltage is shown by the green line.

1) Resistive Λoad

Figure 9 displays the outcomes of the fluctuations in the source voltage, which was maintained at a stable level of 220 V, but subsequently decreased to 180 V and 198 V at 0.04 seconds and 0.1 seconds, respectively. The results demonstrate that the load voltage exhibits a rapid response to the reference voltage. Specifically, at 0.04 seconds, the load voltage reaches the reference voltage after a quarter of a cycle. By 0.1 seconds, the load voltage has rapidly converged with the reference voltage. The input current of the AC-AC converter is sinusoidal and proportional to the amount of voltage compensation required. In the case of a low source voltage, the Total Harmonic Distortion (THD) is observed to be low, with a value of 1.47%.

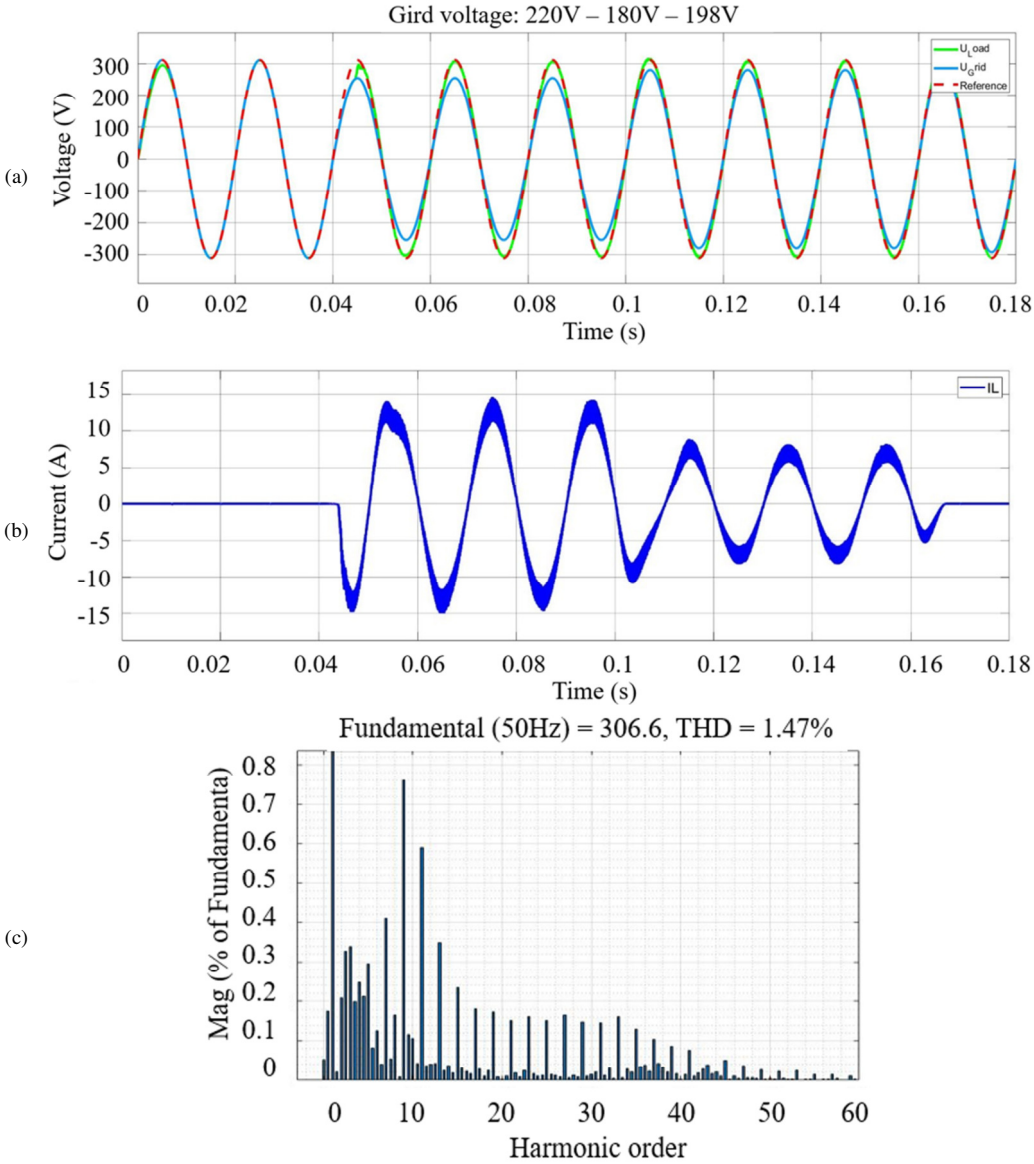

Fig. 9. System response when the source voltage fluctuates: stable - low - low (220 V – 180 V -198 V): (a) load voltage response, (b) Input current of AC-AC converter, (c) THD analysis of load voltage when the source voltage is low.

Figure 10 presents the simulation results for a fluctuating source voltage, demonstrating a transition from a stable to a low voltage state and subsequently back to a stable state. The initial source voltage is stable at 220 V. At 0.04 seconds, it drops below 150 V and subsequently returns to 220 V at 0.14 seconds. The simulation results indicate that the AC-AC converter is operational only when the source voltage is below 220 V. As observed in Figure 10 (b), the input current remains sinusoidal throughout these periods. The load voltage exhibits a response time of less than one-quarter of the grid voltage cycle, demonstrating a tracking of the reference voltage. When the source voltage is low, the THD is minimal, at 1.85%.

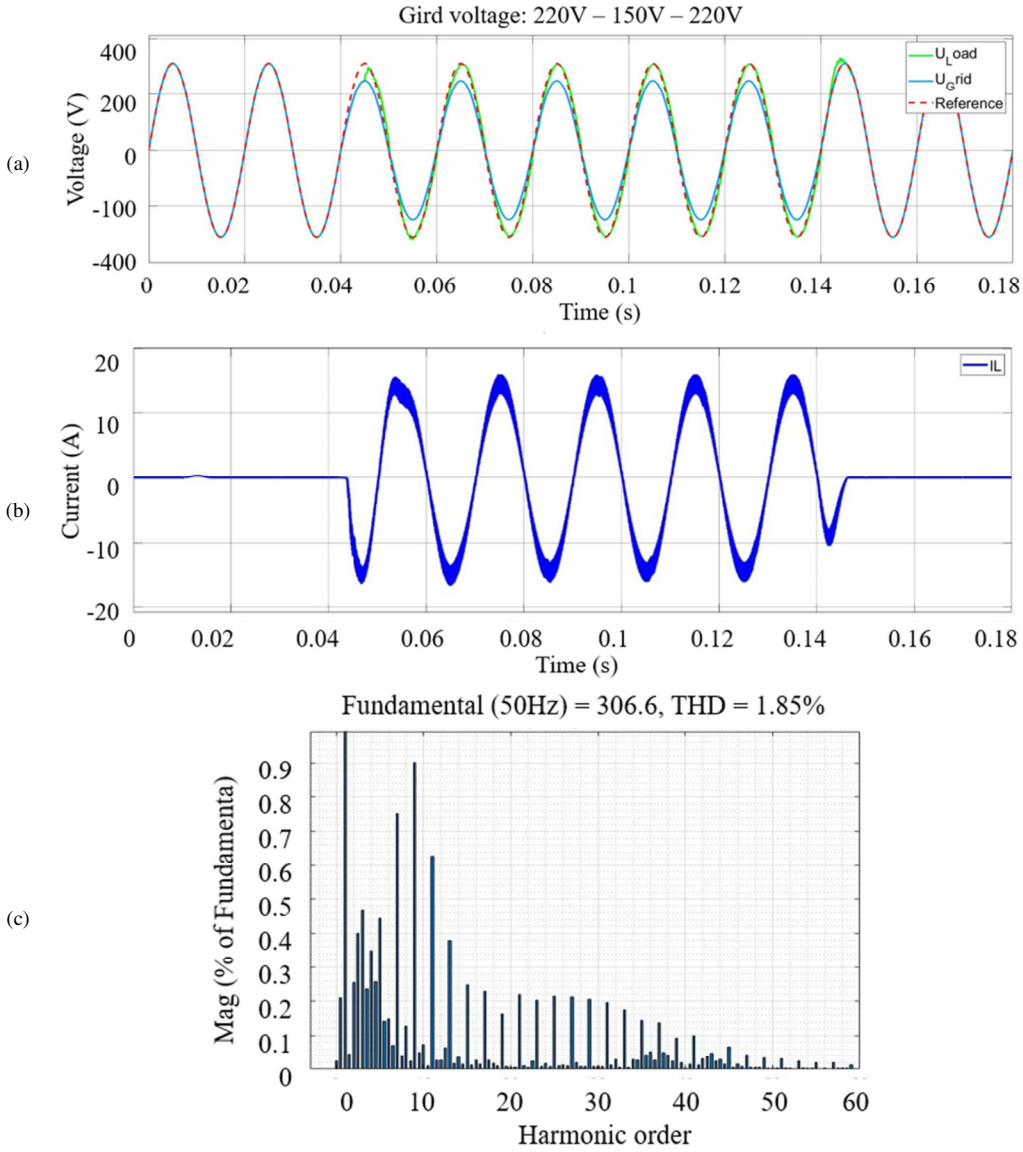

Fig. 10. System response when the source voltage fluctuates: stable - low - stable (220 V – 150 V – 220 V): (a) load voltage response, (b) Input current of AC-AC converter, (c) THD analysis of load voltage when the source voltage is low.

Figure 11 presents the simulation results when the source voltage fluctuates between stable, low, and high levels. The source voltage begins at a stable 220 V and subsequently declines below 175 V at 0.04 seconds before exhibiting an increase to 265 V at 0.14 seconds. Upon the decline of the source voltage to 175 V at 0.04 seconds, the load voltage exhibits alignment with the reference voltage after a quarter cycle of the grid voltage. Conversely, upon the subsequent rise of the source voltage to 267 V at 0.14 seconds, the load voltage demonstrates alignment with the reference after a half cycle of the grid voltage. When the source voltage is elevated, the THD is observed to be 2.26%.

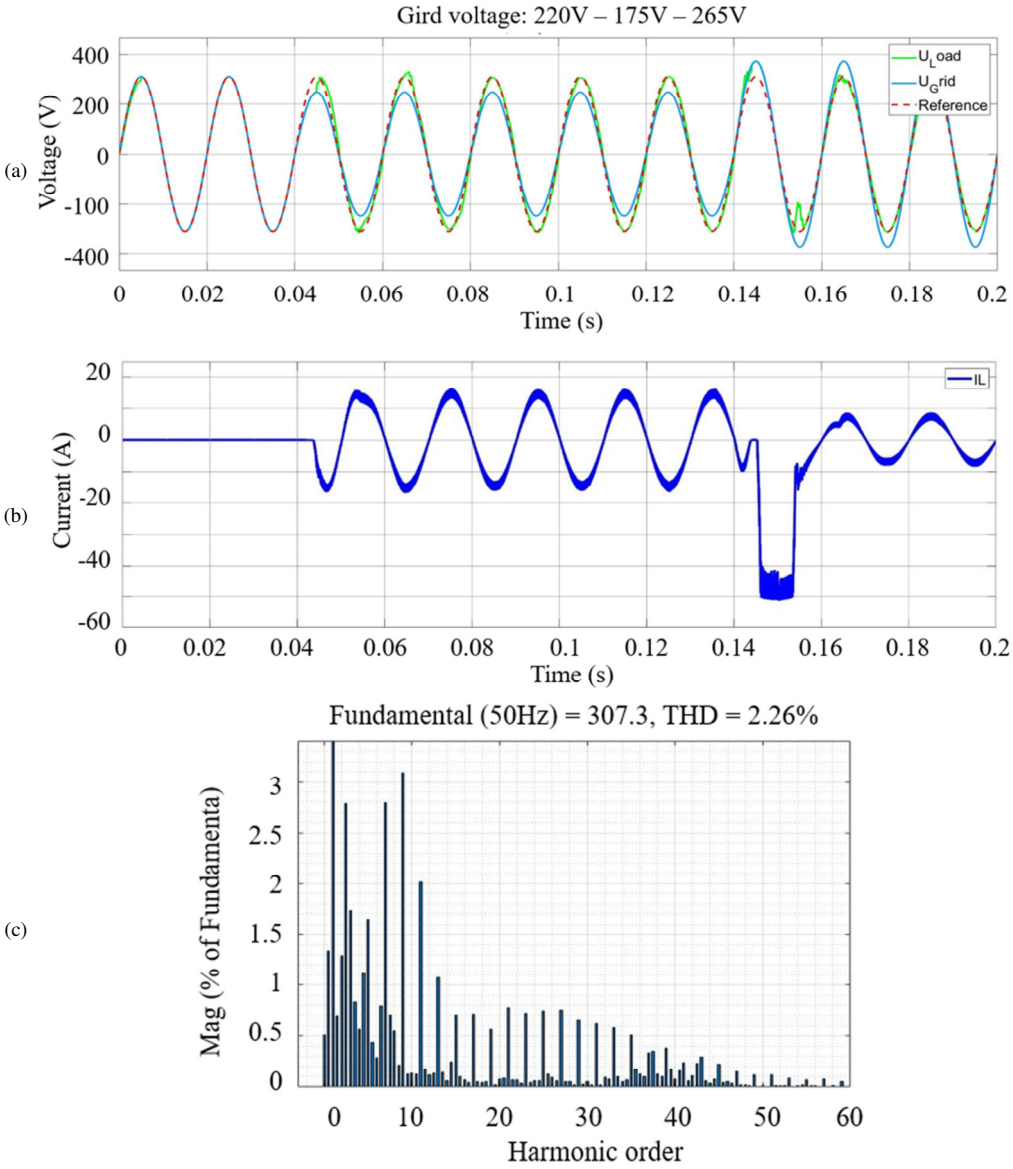

Fig. 11. System response when source voltage fluctuates: stable – low - high (220 V – 175 V – 265 V): (a) load voltage response, (b) input current of AC-AC converter, (c) THD analysis of load voltage when the source voltage is low.

2) Resistive - Inductive Load

The simulation results for inductive-resistive loads with a power factor of 0.84 are presented in Figure 12. The source voltage exhibits the following fluctuations: a stable value of 220 V, a low value of 175 V, a high value of 265 V, and a low value of 187 V, occurring at 0.04 seconds, 0.14 seconds, and 0.24 seconds, respectively. The response times for these fluctuations are 1/4 cycle of the source voltage when the voltage drops to 175 V at 0.04 seconds, 1/2 cycle when it rises to 265 V at 0.14 seconds, and 1/2 cycle when it drops to 187 V at 0.24 seconds. During transient periods, the THD is slightly elevated, reaching 7.4%. However, this occurs within a single grid cycle. In a steady state, the THD is relatively low, at 1.71%. The voltage waveform exhibits a high degree of similarity to the reference signal. The Power Factor (PF) remains above 0.9 throughout.

3) Resistive - Capacitive Load

The simulation results for capacitive-resistive loads with a power factor of 0.84 are depicted in Figure 13. The source voltage exhibits fluctuations, commencing with a stable value of 220 V. The voltage then declines to 175 V at 0.04 seconds, rises to 265 V at 0.14 seconds, and subsequently decreases to 187 V at 0.24 seconds. As with other types of loads, the load voltage exhibits a close tracking of the reference voltage, with a rapid response time of less than one-half cycle of the grid voltage. In a steady state, the THD is low, at 1.71%. During a single system transient cycle, the THD increased to 7.83%.

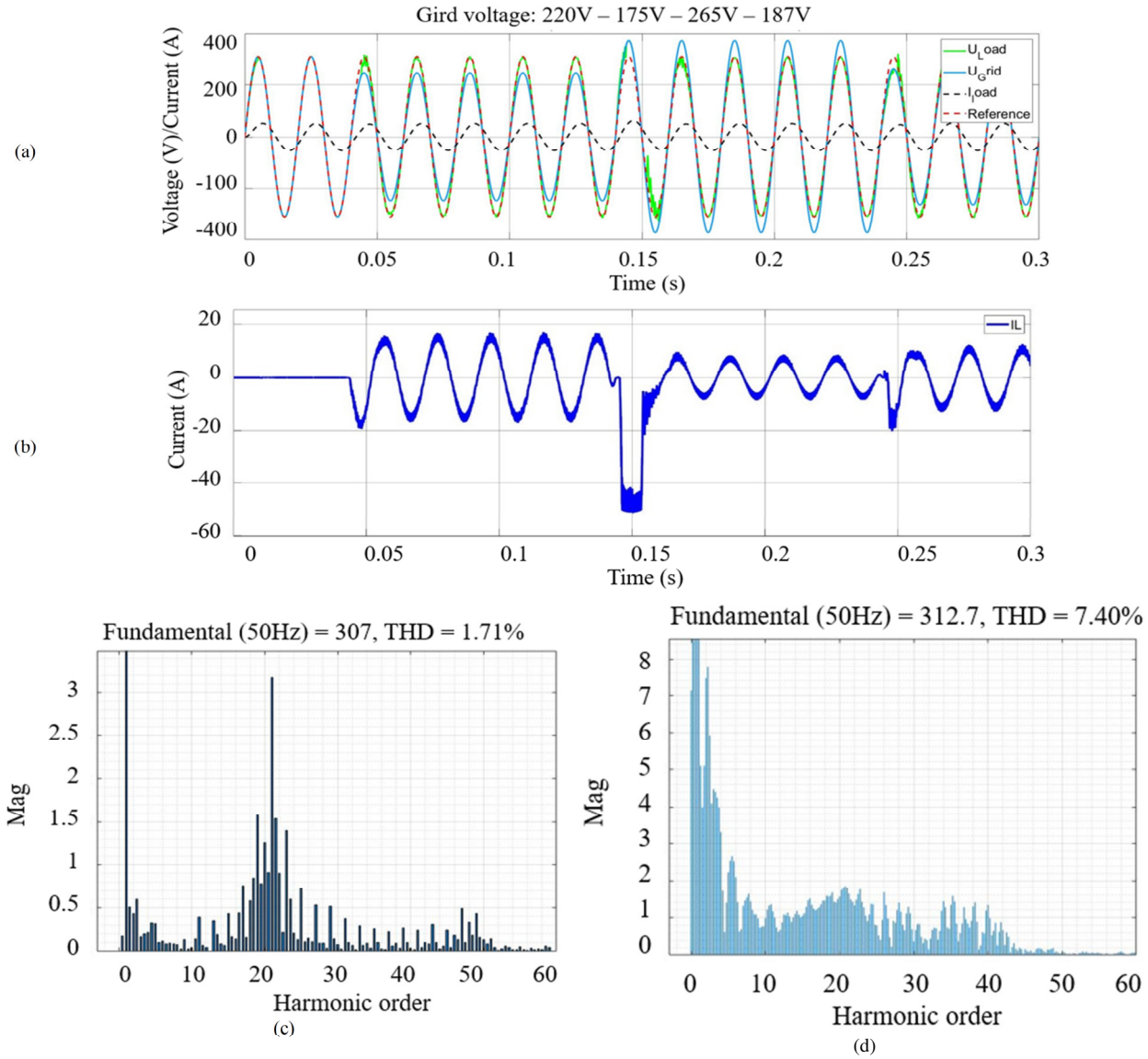

Fig. 12. System response when source voltage fluctuates: stable – low – high – low (220 V – 175 V– 265 V – 187 V): (a) load voltage/current response, (b) input current of AC-AC converter, (c) THD analysis of load voltage when source voltage is stably, (d) THD analysis of load voltage in one system transient cycle.

4) Nonlinear Loads

The simulation results for nonlinear loads, specifically the rectifier diode bridge and capacitor, are presented in Figure 14. The load voltage exhibits a high degree of correlation with the reference voltage. The response time is typically rapid, frequently less than one-quarter of a cycle of the grid voltage. However, when the supply voltage fluctuates between 175 V and 265 V, alterations in the conduction state of the TRIACs give rise to transformer transients, which in turn result in a diminished response time of approximately 1/2 cycle of the supply voltage. During transient events, the THD is observed to be slightly elevated, reaching 9.71%. However, this occurs within the confines of a single grid cycle. In a steady state, the THD is 4.4%, which is within the acceptable range for such heavy nonlinear loads. Although there are minor fluctuations in the load voltage during power fluctuations, these are within acceptable limits.

The analysis of the aforementioned simulation results indicates that when the source voltage fluctuates, the load voltage consistently aligns with the reference voltage. The response time is frequently less than one-half of the grid voltage cycle, and in a stable state, the THD remains consistently low (at its maximum, 4.4%). The results demonstrate the efficacy and superior quality of the controller in maintaining voltage stability and minimizing distortion.

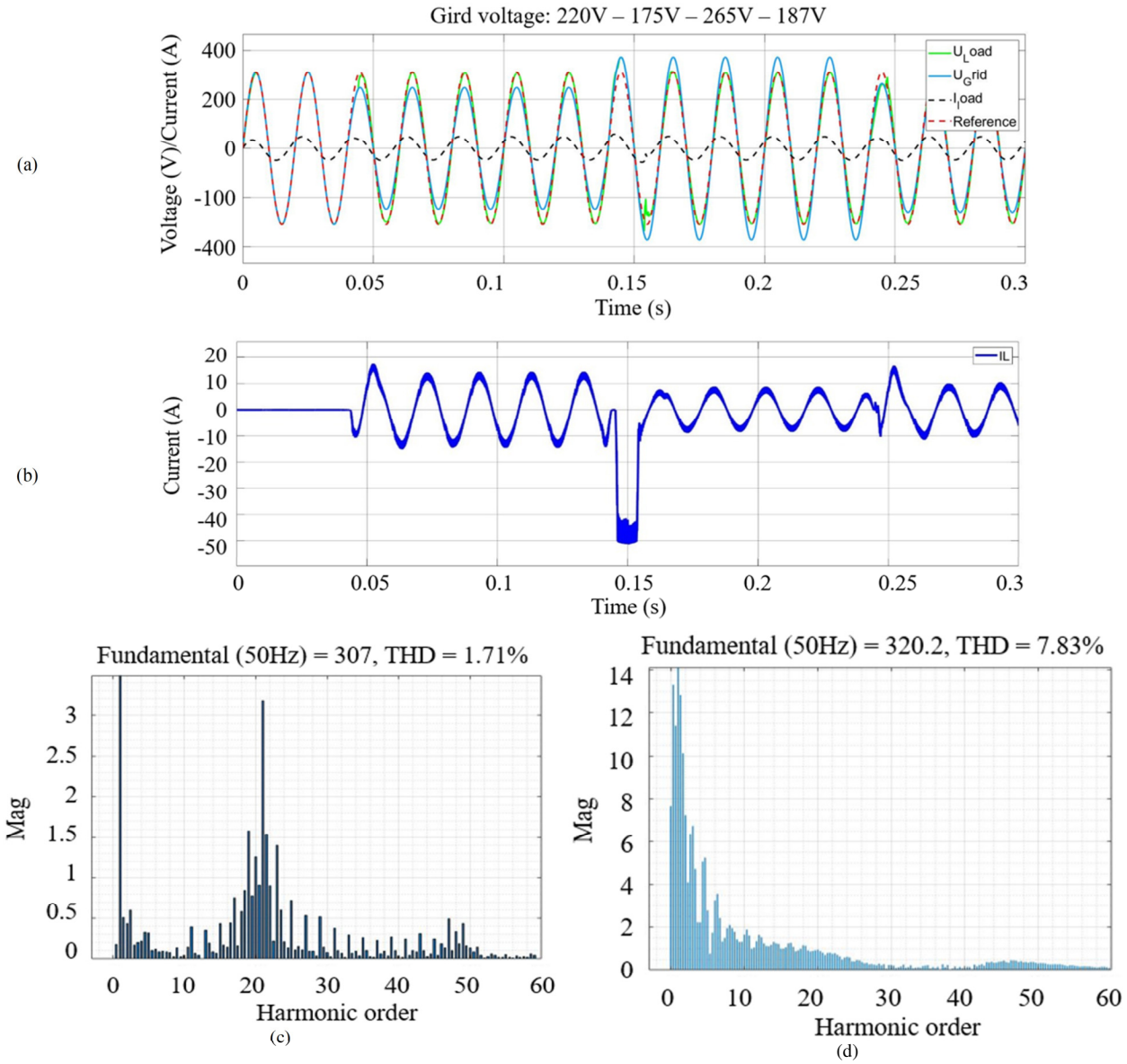

Fig. 13. System response when source voltage fluctuates: stable – low – high – low (220 V – 175 V– 265 V – 187 V): (a) load voltage/current response, (b) input current of AC-AC converter, (c) THD analysis of load voltage when source voltage is stably, (d) THD analysis of load voltage in one system transient cycle.

B. Experimental Results

An experimental model of a 10 kVA electronic voltage stabilizer has been created and is illustrated in Figure 15. The model incorporates an AC-AC converter, a TRIAC H-bridge, a microcontroller (STM32F103C8T6 kit), and a compensating transformer. The initial step involved testing the turn-on signals for the IGBTs in the AC-AC converter. When the modulation factor (D) is set to 0.3, the results, as presented in Figure 16, corroborate that the IGBT turn-on signal waveforms align with the theoretical analysis presented earlier and fulfill the system requirements. It is permissible for the load voltage to fluctuate within a range of ±5% of the reference voltage (equivalent to ±10 VAC). Consequently, when the source voltage fluctuates between 210 V and 230 V, the voltage compensator remains inactive, and the load voltage is directly connected to the source through the bypass. To assess the efficacy of the electronic voltage stabilizer, a series of tests were conducted under diverse source voltage conditions and with varying load types, as detailed below. The subsequent experimental results are presented by a plot of the source voltage (u_s) on the y-axis and the load voltage (u_L) on the x-axis. The red line represents the source voltage, while the blue line represents the load voltage.

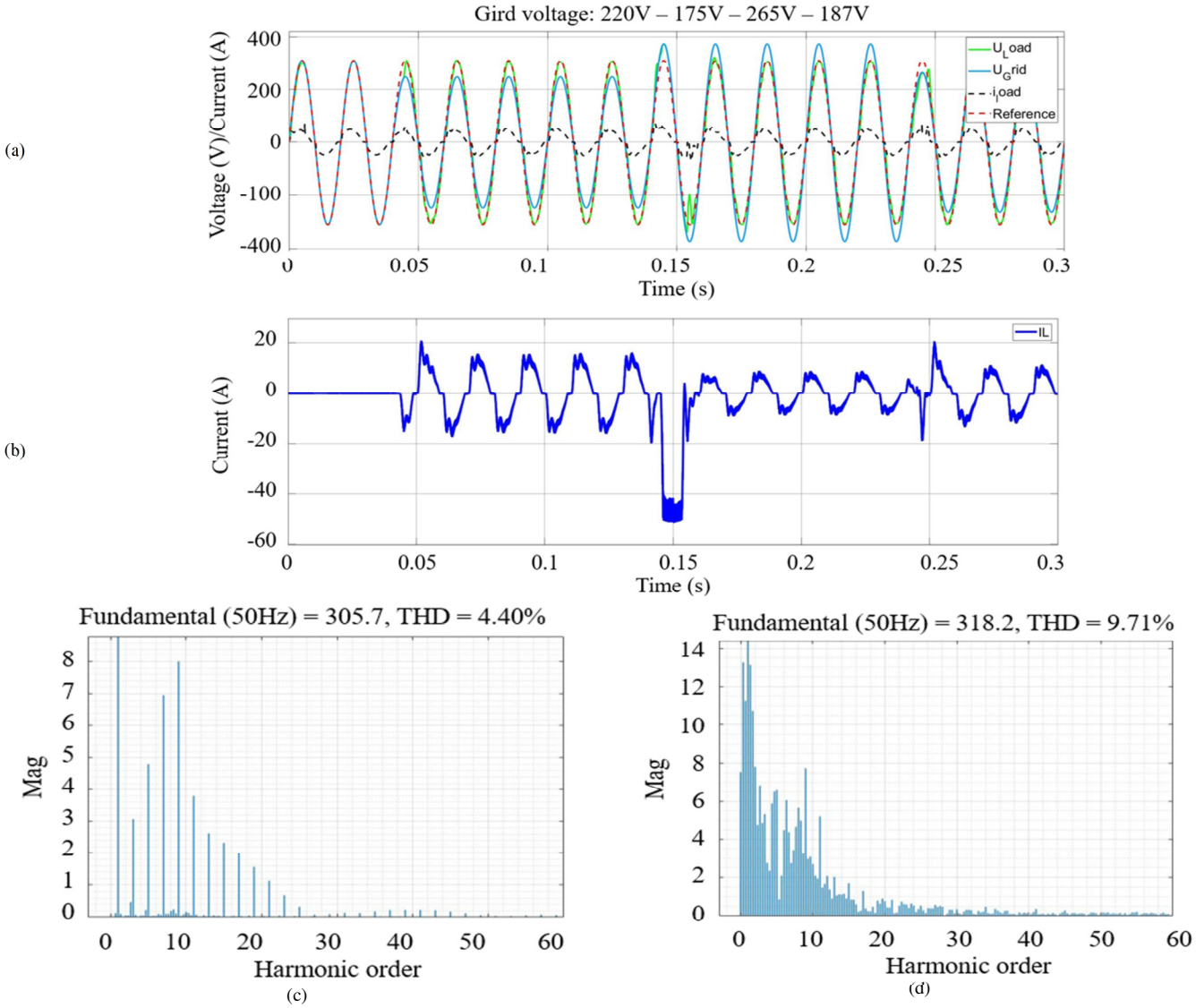

Fig. 14. System response when source voltage fluctuates: stable – low – high – low (220 V – 175 V– 265 V – 187 V): (a) load voltage/current response, (b) input current of AC-AC converter, (c) THD analysis of load voltage when source voltage is stably, (d) THD analysis of load voltage in one system transient cycle.

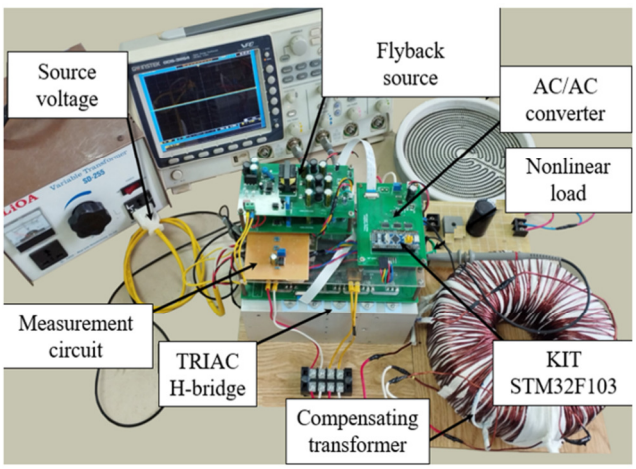

Fig. 15. Experimental model of automatic voltage stabilizer.

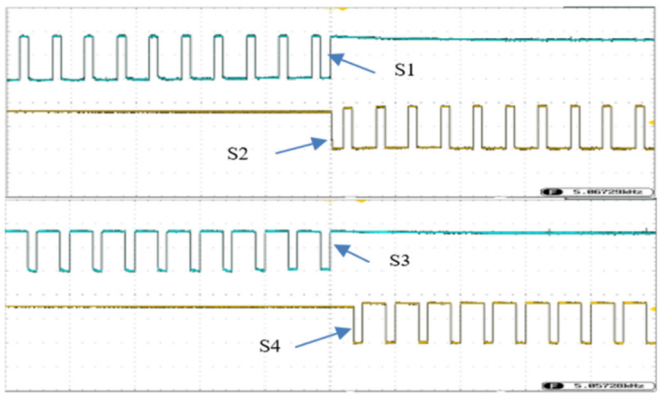

Fig. 16. Turn on/off the signal of IGBTs.

1) Resistive Load

When the source voltage is stable but outside the required limits, the resulting experimental data are presented in Figures 17 and 18. Figures 17 (a) and 18 (a) illustrate the load voltage response when the source voltage is below and above the requisite level, respectively. In both instances, the load voltage maintains a stable RMS value of 220 V and remains in phase with the source voltage. The THD for these conditions is 4.14% and 4.17%, as presented in Figures 17 (b) and Figure 18 (b), respectively. As portrayed in Figure 19, the THD of the source voltage, which serves as a reference, is 3.95%. In the event that the input source is assumed to be ideal, with a THD of 0%, the system's THD response is approximately 0.2%. This suggests that the electronic voltage stabilizer offers a high-quality response with minimal distortion. The results of the experiment conducted with an unstable source voltage are portrayed in Figure 20. Figure 20 (a) depicts a fluctuation in the source voltage, which initially reaches a low level of 190 V before rising to 230 V. Figure 20 (b) displays the scenario in which the source voltage rises from 230 V to 280 V, while Figure 20 (c) exhibits the source voltage declining from a high level (290 V) to a stable level of 230 V. The results demonstrate that in all cases, the load voltage consistently remains at the stable, permissible value of 230 V, with no distortion and in phase with the supply voltage. The response time is rapid, with the load voltage reaching the requisite value with minimal latency, as shown in Figure 20 (a), after a brief interval in Figure 20 (b), and Figure 20 (c).

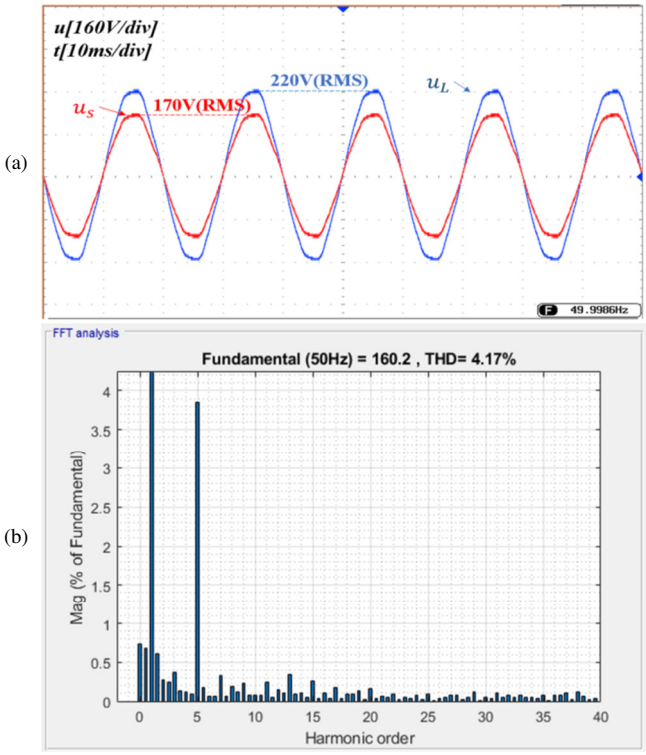

Fig. 17. System response when the source voltage (170 VAC) is low, and the load is resistive: (a) response of output voltage, (b) THD of output voltage (4.17%).

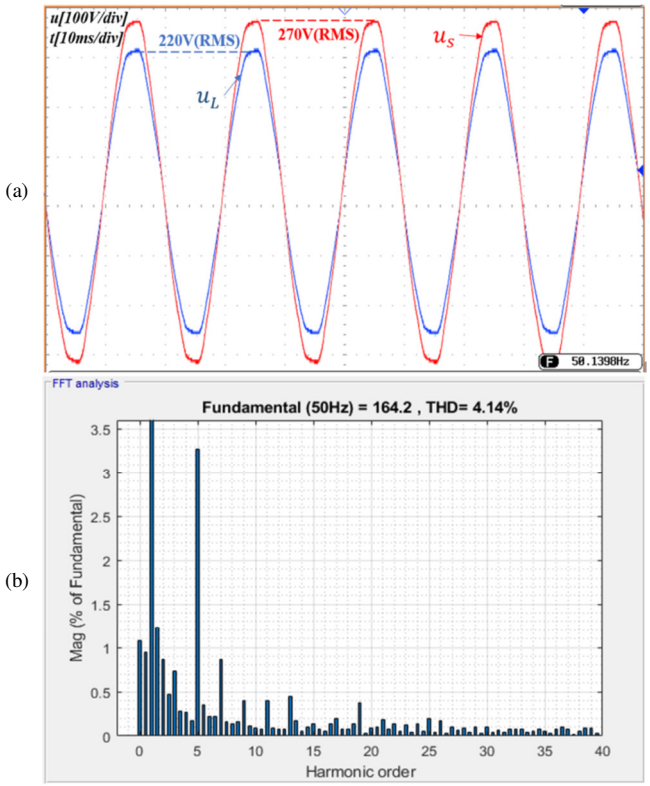

Fig. 18. System response when the source voltage (270 VAC) is high, and the load is resistive: (a) response of output voltage, (b) THD of output voltage (4.14%).

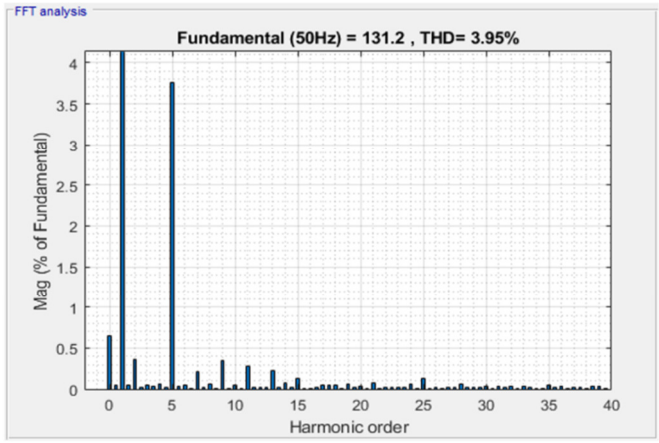

Fig. 19. THD of source voltage with frequency 50Hz (3.95%).

2) NonlinearLoad

The experimental results with nonlinear load when the source voltage fluctuates are shown in Figures 21-23. Figures 21 and 22 illustrate the system response when the source voltage is below and above the requisite voltage level, respectively. In both scenarios, the experimental outcomes demonstrate that the output voltage maintains a stable RMS value of 220 V, and remains in phase alignment with the source voltage. The THD of the load voltage is 5.72% for a source voltage of 160 V, and 5.38% for a source voltage of 270 V. The load voltage exhibits a high THD due to the high THD of

the source (3.95%). In the absence of any distortion in the source (THD = 0%), the automatic voltage stabilizer's THD response is 1.77% and 1.43%, respectively. The system's response quality is satisfactory.

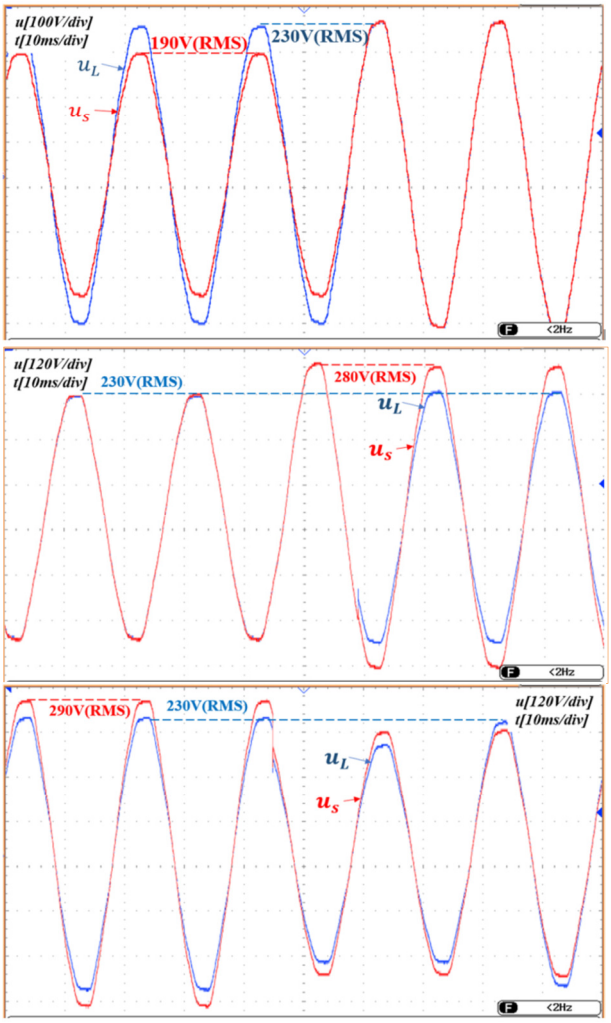

Fig. 20. Load voltage response when source voltage fluctuates, resistive load: (a) low – stable (190 VAC – 230 VAC), (b) stable-high (230 VAC – 280 VAC), (c) high – stable (290 VAC – 230 VAC).

As shown in Figure 23, the load voltage response is observed to fluctuate in conjunction with fluctuations in the source voltage. Figure 23 (a) presents the response of the load voltage when the source voltage undergoes fluctuations from a low level of 170 V to a stable level of 215 V, which remains within the specified limit. The findings indicate that the load voltage remains consistently stable at 215 V. Figure 23 (b) showcases the load voltage response in the event of a fluctuation in the source voltage, from a stable level of 215 V to a lower level of 180 V. The load voltage is maintained at a constant 215 V. The response time is less than one-half of a grid voltage cycle.

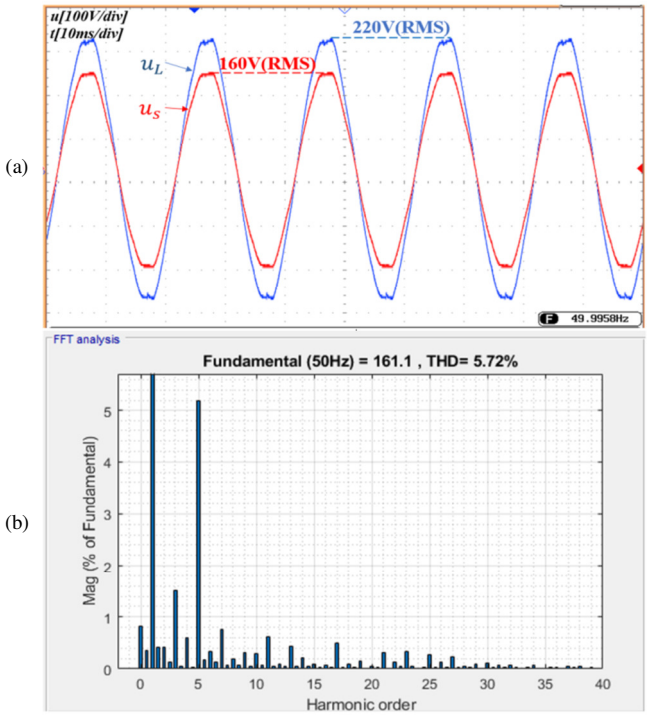

Fig. 21. System response when the source voltage (160 V) is low, and the load is nonlinear: (a) response of output voltage, (b) THD of output voltage (5.72%).

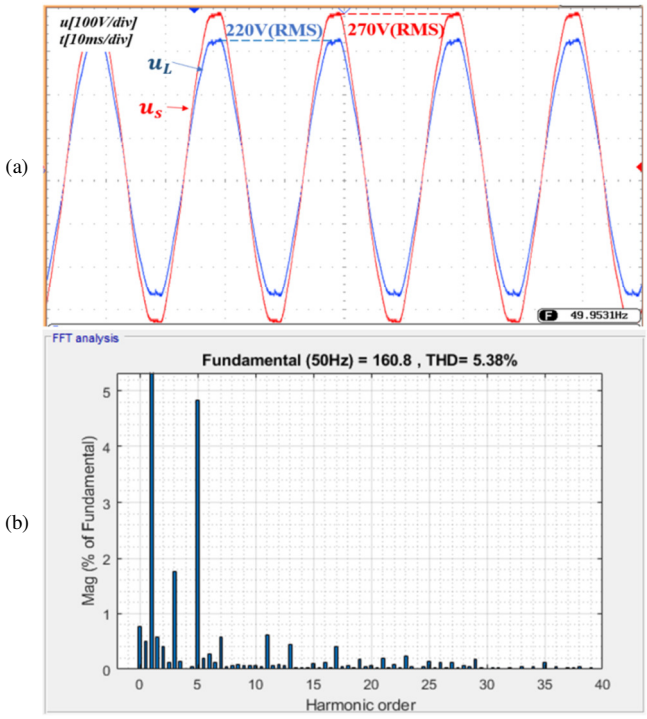

Fig. 22. System response when the source voltage (270 V) is high, and the load is nonlinear: (a) response of output voltage, (b) THD of output voltage (5.38%).

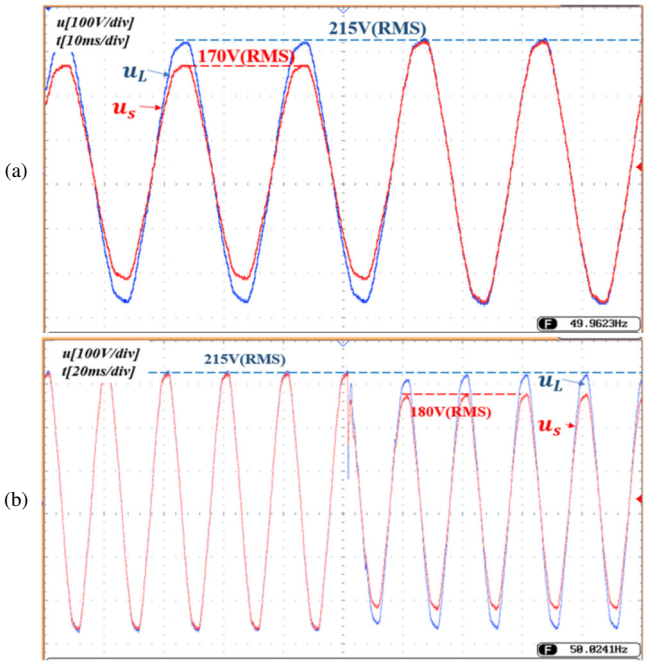

Fig. 23. Load voltage response in the case of nonlinear load when the source voltage fluctuates: (a) low – stable (170 VAC – 215 VAC), (b) stable – low (215 VAC – 180 VAC).

The experimental results demonstrate that the electronic voltage stabilizer exhibits a rapid response time (less than one-half cycle of the grid voltage), maintains a voltage on the load within the allowable limit (±5%), and exhibits a THD of less than 2% when the system is operating stably. In order to illustrate the advantages of the proposed design, a comparison is presented between the results obtained and those of previous studies on voltage stabilizers with comparable structures. The results of the comparison are presented in Table II. With regard to the structure of the voltage stabilizer, these studies use an AC/AC converter with four semiconductor switches, with the primary distinction being in the configuration of the compensation transformer.

The compensation transformer in [18, 19] employs two secondary windings, whereas this study's proposal uses a single secondary winding. Furthermore, they use two bidirectional switches to reverse the compensation voltage polarity, whereas the particular proposal employs four bidirectional switching devices (TRIACs). In terms of control structure, authors in [18] employed an I and PI controller, authors in [19] used an LQR controller, while the current research employs a combination of feedforward and feedback controllers. Regarding, the time required for the measurement and calculation of the RMS value of the source and load voltage, authors in [18] required 0.3 seconds for initialization. The proposed method requires only 0.01 seconds to measure and calculate the RMS value. With the same source frequency and required output voltage level, the introduced design permits a wider input voltage fluctuation range while achieving a markedly faster response time (less than half a cycle in simulations). The aforementioned comparative analysis demonstrates the superiority of the proposed design.

IV. CONCLUSIONS

The objective of this paper is to present a novel control design method for electronic voltage stabilizers. The proposed configuration of the electronic voltage stabilizer incorporates an AC-AC converter, a compensation transformer, and a TRIAC H-bridge for phase inversion.

TABLE II. COMPARISON RESULTS

Criteria	**[18]**	**[19]**	**Proposed design**
AC/AC converter	Yes	Yes	Yes
No. of switches	4	4	4
Transformer	Two secondary windings	Two secondary windings	One secondary windings
Adjust compensation voltage	Yes	Yes	Yes
Controller	I and PI	LQR	Feedfoward and feedback
RMS measurement/ calculation time:	0.3 s (initial)	-	< 0.01 s
Capacity	2.2 kVA	1 kW	10 kVA
Input voltage	220V ± 10%	200 V ÷ 240 V	150 V ÷ 290 V
Output voltage	220 V	220 V	220 V ± 5%
Frequency	50 Hz	50 Hz	50 Hz
Response time (simulation)	0.1 s	0.05 s	< 1/2 cycle grid voltage (< 10 ms)
THD (in simulation and steady state)	1.64% (RL load)	-	1.71% (RL load)
THD (in experimental and steady state)	-	-	0,2% (R load) 1,77% (Nonlinear load)

The current paper puts forth the use of the state-space averaging method for system modeling and proposes the combination of feed-forward and feedback controllers as a means of achieving high accuracy and a fast response time. Furthermore, a moving average algorithm is proposed for measuring the Root Mean Square (RMS) value of the source voltage and load, resulting in faster measurement and calculation times (approximately 0.01 seconds). This is a notable improvement over the measurement methods used in other similar studies. A 10 kVA single-phase electronic voltage stabilizer model was constructed in a laboratory setting to verify the proposed method. The results demonstrated that when the source voltage fluctuates between 150 V and 290 V under varying load conditions, the voltage across the load remains within the specified range of 220 V ± 5%. The response time of the stabilizer is notably rapid, exhibiting a significantly shorter latency than that of comparable designs. In simulations, the response time is observed to be approximately half a cycle, while in experiments, it is seen to be approximately one cycle. The total harmonic distortion in the experimental results is relatively low, at approximately 0.2% for a purely resistive load and around 1.77% for a nonlinear load.

ACKNOWLEDGMENT

This research is funded by the Ministry of Industry and Trade of the Socialist Republic of Vietnam under the project number ĐT KHCN.049/23.

REFERENCES

[1] S. Z. Djokic, J. Desmet, G. Vanalme, J. V. Milanovic, and K. Stockman, "Sensitivity of personal computers to voltage sags and short

interruptions," *IEEE Transactions on Power Delivery*, vol. 20, no. 1, pp. 375–383, Jan. 2005, https://doi.org/10.1109/TPWRD.2004.837828.

[2] L. Tang, Y. Han, P. Yang, C. Wang, and A. S. Zalhaf, "A review of voltage sag control measures and equipment in power systems," *Energy Reports*, vol. 8, pp. 207–216, Nov. 2022, https://doi.org/10.1016/j.egyr.2022.05.158.

[3] L. Jinbing, Y. Guochao, S. Zhezheng, D. Siying, and W. Yudan, "Overview and analysis of voltage sag mitigation measures," in *2021 Power System and Green Energy Conference (PSGEC)*, Shanghai, China, Aug. 2021, pp. 262–268, https://doi.org/10.1109/PSGEC51302.2021.9541716.

[4] A. M. Rauf and V. Khadkikar, "An Enhanced Voltage Sag Compensation Scheme for Dynamic Voltage Restorer," *IEEE Transactions on Industrial Electronics*, vol. 62, no. 5, pp. 2683–2692, May 2015, https://doi.org/10.1109/TIE.2014.2362096.

[5] S. Subramanian and M. K. Mishra, "Interphase AC–AC Topology for Voltage Sag Supporter,"*IEEE Transactions on Power Electronics*, vol. 25, no. 2, pp. 514–518, Feb. 2010, https://doi.org/10.1109/TPEL.2009.2027601.

[6] E. C. Aeloiza, P. N. Enjeti, O. C. Montero, and L. A. Moran, "Analysis and design of a new voltage sag compensator for critical loads in electrical power distribution systems," in *Conference Record of the 2002 IEEE Industry Applications Conference. 37th IAS Annual Meeting (Cat. No.02CH37344)*, Pittsburgh, PA, USA, Oct. 2002, vol. 2, pp. 911–916 vol.2, https://doi.org/10.1109/IAS.2002.1042667.

[7] V. H. Nguyen, H. Nguyen, M. T. Cao, and K. H. Le, "Performance Comparison between PSO and GA in Improving Dynamic Voltage Stability in ANFIS Controllers for STATCOM," *Engineering, Technology & Applied Science Research*, vol. 9, no. 6, pp. 4863–4869, Dec. 2019, https://doi.org/10.48084/etasr.3032.

[8] P. D. Chung, "Voltage Enhancement on DFIG Based Wind Farm Terminal During Grid Faults," *Engineering, Technology & Applied Science Research*, vol. 9, no. 5, pp. 4783–4788, Oct. 2019, https://doi.org/10.48084/etasr.3117.

[9] D. D. Tung and N. M. Khoa, "An Arduino-Based System for Monitoring and Protecting Overvoltage and Undervoltage," *Engineering, Technology & Applied Science Research*, vol. 9, no. 3, pp. 4255–4260, Jun. 2019, https://doi.org/10.48084/etasr.2832.

[10] D. K. Singh, J. Singh, and R. R. Ravela, "Design and Performance Study of Cost Effective Smart Servo Controlled Automatic Voltage Stabilizer," in *2020 International Conference on Electrical and Electronics Engineering (ICE3)*, Gorakhpur, India, Feb. 2020, pp. 211–215, https://doi.org/10.1109/ICE348803.2020.9122815.

[11] J. Kaniewski, Z. Fedyczak, and G. Benysek, "AC Voltage Sag/Swell Compensator Based on Three-Phase Hybrid Transformer With Buck-Boost Matrix-Reactance Chopper," *IEEE Transactions on Industrial Electronics*, vol. 61, no. 8, pp. 3835–3846, Aug. 2014, https://doi.org/10.1109/TIE.2013.2288202.

[12] P. Eswaran and M. Nishanth, "Design of fuzzy logic controller for customized servo voltage stabilizer," in *2015 2nd International Conference on Electronics and Communication Systems (ICECS)*, Coimbatore, India, Feb. 2015, pp. 103–106, https://doi.org/10.1109/ECS.2015.7124735.

[13] P. N. Wijesooriya, N. Kularatna, and D. A. Steyn-Ross, "Efficiency Enhancements to a Linear AC Voltage Regulator: Multiwinding Versus Multitransformer Design," *IEEE Journal of Emerging and Selected Topics in Industrial Electronics*, vol. 1, no. 2, pp. 192–199, Oct. 2020, https://doi.org/10.1109/JESTIE.2020.3003350.

[14] K. N. Tarchanidis, J. N. Lygouras, and P. Botsaris, "Voltage Stabilizer Based on SPWM technique Using Microcontroller," *Journal of Engineering Science and Technology Review*, vol. 6, no. 1, pp. 38–43, Feb. 2013, https://doi.org/10.25103/jestr.061.08.

[15] Y. Zhu, W. Hu, Z. Wang, and X. Ma, "Single-phase on-line uninterruptible power supply with low load regulation," in *2021 IEEE International Conference on Power Electronics, Computer Applications (ICPECA)*, Shenyang, China, Jan. 2021, pp. 615–619, https://doi.org/10.1109/ICPECA51329.2021.9362585.

[16] C.-Y. Park, J.-M. Kwon, and B.-H. Kwon, "Automatic voltage regulator based on series voltage compensation with ac chopper," *IET Power Electronics*, vol. 5, no. 6, pp. 719–725, Jul. 2012, https://doi.org/10.1049/iet-pel.2011.0337.

[17] M. R. Hajimoradi and H. Mokhtari, "AC voltage regulator based on AC/AC buck converter," in *2016 7th Power Electronics and Drive Systems Technologies Conference (PEDSTC)*, Tehran, Iran, Feb. 2016, pp. 140–146, https://doi.org/10.1109/PEDSTC.2016.7556852.

[18] H. Liu, J. Wang, and O. Kiselychnyk, "Mathematical Modeling and Control of a Cost Effective AC Voltage Stabilizer," *IEEE Transactions on Power Electronics*, vol. 31, no. 11, pp. 8007–8016, Nov. 2016, https://doi.org/10.1109/TPEL.2015.2514180.

[19] B. Kim, S. Am, P. Chrin, E. Boulaud, and E. Boisaubert, "Study of the Control of an AC Voltage Stabilizer Using LQR and Anti-windup," in *2020 International Symposium on Power Electronics, Electrical Drives, Automation and Motion (SPEEDAM)*, Sorrento, Italy, Jun. 2020, pp. 623–627, https://doi.org/10.1109/SPEEDAM48782.2020.9161967.

[20] U. A. Khan, A. A. Khan, H. Cha, H.-G. Kim, J. Kim, and J.-W. Baek, "Dual-Buck AC–AC Converter With Inverting and Non-Inverting Operations," *IEEE Transactions on Power Electronics*, vol. 33, no. 11, pp. 9432–9443, Nov. 2018, https://doi.org/10.1109/TPEL.2018.2799490.

[21] Y.-K. Chen, X.-Z. Qiu, Y.-C. Wu, and C.-C. Song, "Compensation of Voltage Sags and Swells Using Dynamic Voltage Restorer Based on Bi-Directional H-Bridge AC/AC Converter," *Processes*, vol. 9, no. 9, Sep. 2021, Art. no. 1541, https://doi.org/10.3390/pr9091541.

[22] Z. Aleem, H.-K. Yang, H. F. Ahmed, S. L. Winberg, and J.-W. Park, "A Class of Single-Phase Z-Source AC–AC Converters With Magnetic Coupling and Safe-Commutation Strategy," *IEEE Transactions on Industrial Electronics*, vol. 68, no. 9, pp. 8104–8115, Sep. 2021, https://doi.org/10.1109/TIE.2020.3018058.